

Study of the (${}^6\text{Li}, {}^6\text{He}$) reactions*

W. R. Wharton[†] and P. T. Debevec[‡]

Argonne National Laboratory, Argonne, Illinois 60439

(Received 3 February 1975)

We have measured and analyzed angular distributions of (${}^6\text{Li}, {}^6\text{He}$) reactions at $E_{\text{lab}} \sim 34$ MeV on targets between $A = 6$ and $A = 48$. The analysis indicates that the (${}^6\text{Li}, {}^6\text{He}$) reaction has sizable contributions from multistep processes except possibly for transitions of zero angular momentum transfer ($L = 0$) near closed shells. The $L = 0$ partial cross sections of the (${}^6\text{Li}, {}^6\text{He}$) reaction are correlated with the known Gamow-Teller strength obtained from β -decay measurements, except for a smoothly target-dependent uncorrelated factor which makes the (${}^6\text{Li}, {}^6\text{He}$) $L = 0$ cross sections too large in the middle of the s - d shell. The (${}^6\text{Li}, {}^6\text{He}$) reactions should be useful in studying the distribution of Gamow-Teller strength in nuclei.

[NUCLEAR REACTIONS ${}^{18}\text{O}({}^6\text{Li}, {}^6\text{He})$, ${}^{30}\text{Si}({}^6\text{Li}, {}^6\text{He})$, ${}^{34}\text{S}({}^6\text{Li}, {}^6\text{He})$, $E = 32$ MeV; ${}^{42,44,48}\text{Ca}({}^6\text{Li}, {}^6\text{He})$, $E = 34$ MeV; measured $\sigma(E_{\text{He}}, \theta)$, systematic DWBA analysis includes ${}^6\text{Li}({}^6\text{Li}, {}^6\text{He})$ and ${}^{26}\text{Mg}({}^6\text{Li}, {}^6\text{He})$.]

I. INTRODUCTION

This is a report of a systematic study of the (${}^6\text{Li}, {}^6\text{He}$) reactions; their reaction mechanism and their potential value as a spectroscopic tool. The (${}^6\text{Li}, {}^6\text{He}$) reaction replaces a proton with a neutron and therefore can be classified as a charge-exchange reaction. Charge-exchange reactions became an interesting topic twelve years ago with the first identification of isobaric analog states in heavy nuclei using the (p, n) reaction.¹ In (p, n) reactions the proton can undergo charge exchange with one of the neutrons in the target by means of the $(\vec{t}_i \cdot \vec{t}_j)$ term in the nucleon-nucleon force. The analog state is strongly populated because it exhausts most of the Fermi strength given by $\langle B || \sum_j t_j || A \rangle$, where the index j sums over the individual nucleons in the initial nucleus A and final nucleus B . It then seemed reasonable that other reduced matrix elements (RME) could be measured, but during the ensuing years neither the (p, n) nor the extensively studied (${}^3\text{He}, t$) reaction has been of much use in measuring RME. The lack of such quantitative spectroscopic information has resulted from difficulties in measuring (p, n) cross sections and complications in the (${}^3\text{He}, t$) reaction mechanism which is often dominated by the two-step neutron pickup-proton stripping process (${}^3\text{He}-\alpha-t$).²

As there is great value in measuring the reduced matrix elements between isobars, it seemed well worth pursuing other charge exchange reactions. Very little study of the (${}^6\text{Li}, {}^6\text{He}$) reaction had been made. Also, the (${}^6\text{Li}, {}^6\text{He}$) reaction must involve a spin transfer as well as a charge transfer and therefore is more selective than

(p, n) or (${}^3\text{He}, t$). Recently, measurements of the ${}^6\text{Li}({}^6\text{Li}, {}^6\text{He}){}^6\text{Be}$ reaction at $E_{\text{lab}} = 32$ and 36 MeV gave encouraging results.³ Both the measured angular distributions and magnitude of the cross section were consistent with the distorted-wave Born-approximation (DWBA) calculations assuming a one-step inelastic interaction. Here a proton in one of the $T = 0$, $J^\pi = 1^+$ ${}^6\text{Li}$ nuclei interacts with a neutron in the other ${}^6\text{Li}$; they exchange their charge and flip their spins forming $T = 1$, $J = 0^+$ final nuclei. Pursuing this reaction further, we have measured the ${}^{18}\text{O}({}^6\text{Li}, {}^6\text{He}){}^{18}\text{F}$, ${}^{30}\text{Si}({}^6\text{Li}, {}^6\text{He}){}^{30}\text{P}$, ${}^{34}\text{S}({}^6\text{Li}, {}^6\text{He}){}^{34}\text{Cl}$ reactions at $E_{\text{lab}} = 32$ MeV and the ${}^{42,44,48}\text{Ca}({}^6\text{Li}, {}^6\text{He}){}^{42,44,48}\text{Sc}$ reactions at 34 MeV, and we have reanalyzed earlier data⁴ on the ${}^{26}\text{Mg}({}^6\text{Li}, {}^6\text{He}){}^{26}\text{Al}$ reaction.

II. EXPERIMENTAL PROCEDURE

Two 4.5 cm long Si-surface-barrier position-sensitive detectors⁵ are placed in the focal plane of the Argonne National Laboratory Enge split-pole spectrograph. The ${}^6\text{He}$ ions are identified according to their energy loss in the detectors, and their energy is determined from their position along the focal plane. The detectors are 500- μm thick and, because the ions enter the detector at a 45° angle, the effective thickness is 700 μm . During our measurements we were interested in ${}^6\text{He}^{++}$ ions with 20 to 30 MeV kinetic energy. The ${}^4\text{He}^{++}$ of the same rigidity have 30 to 45 MeV. The detectors can stop ${}^4\text{He}$ ions of 39 MeV. The ${}^6\text{Li}^{++}$ and ${}^6\text{He}^{++}$ ions have the same rigidity at the same energy and therefore would be indistinguishable. To distinguish them we placed up to 0.1 mm of aluminum foil in front of

the detector to degrade the ${}^6\text{Li}$ energy more than the ${}^6\text{He}$ energy. The foil also slowed down ${}^4\text{He}^{++}$ ions so that they lost nearly their full energy in the detector. A typical particle spectrum is shown in Fig. 1.

The position signal is obtained using analog hardware to divide the E_x signal by the E signal. The position and energy are stored two dimensionally in direct access mode into a 64 000 word memory. The two-dimensional storage allows cleaner ion separation than is indicated by Fig. 1. A typical spectrum is shown for the ${}^{30}\text{Si}({}^6\text{Li}, {}^6\text{He}){}^{30}\text{P}$ reaction in Fig. 2. The spectrum up to 0.8 MeV is taken with one position-sensitive detector and the spectrum between 2.5 and 3.1 MeV is taken simultaneously with a second detector. The energy resolution is better than 30 keV, which is sufficient to resolve the 0^+ state at 0.677 MeV and the 1^+ state at 0.709 MeV. The background between peaks is zero, indicating a clean ${}^6\text{He}$ spectrum.

The magnitude of the cross sections has been determined by calibrating the system with a measurement of the elastic scattering at angles where it is predicted to be larger than 90% Rutherford and normalizing to an optical model calculation. The major error associated with this measurement is the angular calibration of the spectrograph which we determined to within 0.06° by measuring the elastic scattering on each side of

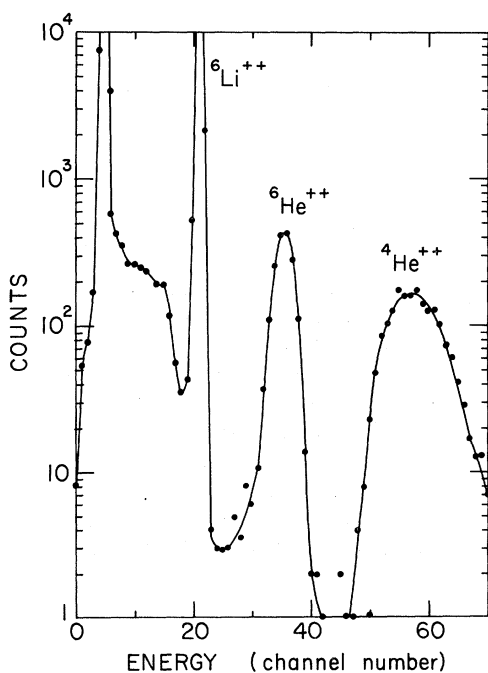


FIG. 1. A typical particle spectrum. This is obtained from the ${}^{44}\text{Ca}({}^6\text{Li}, {}^6\text{He}){}^{44}\text{Sc}$ reaction at $E_{\text{lab}} = 34$ MeV and $\theta_{\text{lab}} = 10^\circ$.

the beam. The errors in the cross sections should be less than 15%; however, our ${}^{48}\text{Ca}({}^6\text{Li}, {}^6\text{He}){}^{48}\text{Sc}$ cross sections are 40% larger than those reported by Gaarde and Kammuri.⁶

The only difficult experimental problem is the low count rate which has four contributing factors. (1) For incident energies of $E_{\text{lab}} \approx 34$ MeV nearly all $({}^6\text{Li}, {}^6\text{He})$ cross sections are less than $200 \mu\text{b}/\text{sr}$. (2) ${}^6\text{Li}$ has a large stopping power requiring thin targets for good energy resolution. (3) ${}^6\text{Li}$ beams are often of lower intensity and less dependable than other commonly used beams. We had 15 to 200 nA of ${}^6\text{Li}^{+++}$ on target; the large range indicates the poor dependability. (4) The narrow oscillations in the diffractive pattern of the angular distributions make it necessary to use narrow solid angles (± 0.2 or $\pm 0.4^\circ$). There are no other serious experimental problems. The study of $({}^6\text{Li}, {}^6\text{He})$ has a distinct advantage over the study of $({}^6\text{Li}, d)$ in that the Q value on ${}^{12}\text{C}$ is -20.9 MeV, which means ${}^{12}\text{C}$ contamination on the target presents no problem.

III. QUASIELASTIC THEORY

One of the primary goals of this work is to study the $({}^6\text{Li}, {}^6\text{He})$ reaction mechanism and in particular to determine to what extent the reaction is quasielastic. We define a quasielastic process as elastic scattering with an additional one-step inelastic interaction between a nucleon in the target and a nucleon in the projectile. It will then be useful to review the general properties of a quasielastic reaction. Using DWBA the transition am-

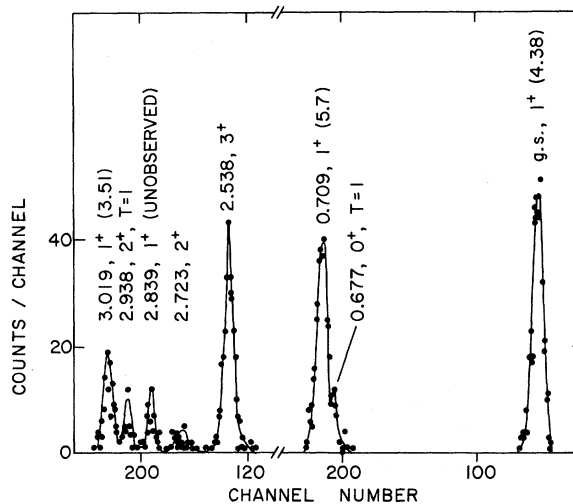


FIG. 2. The ${}^{30}\text{Si}({}^6\text{Li}, {}^6\text{He}){}^{30}\text{P}$ spectrum at $E_{\text{lab}} = 32$ MeV and $\theta_{\text{lab}} = 5^\circ$. Each half of the spectrum is taken from one of two detectors placed in the focal plane of the spectrograph.

plitude for the direct term of a quasielastic reaction $A(a, b)B$ is:

$$T_{ba} = \int \chi_b^-(\vec{R}) F(\vec{R}) \chi_a^+(\vec{R}) d^3R, \quad (1)$$

where the form factor is

$$F(\vec{R}) = \langle Bb | V | Aa \rangle. \quad (2)$$

Equation (2) is a spatial integration over the coordinates of all particles in A and a , and the spin and isospin matrix elements. The interaction V is a two-body interaction between a nucleon, i , in the projectile, a , and a nucleon, j , in the target, A :

$$V = \sum_{i,j} V_{ij}. \quad (3)$$

The radial dependence of the form factor comes from the integration over the spatial coordinates of particles i and j and doing this six-dimensional integration separately, the result is

$$F(\vec{R}) = \sum_{ij} \int G(\vec{r}_i, \vec{r}_j) d\vec{r}_i d\vec{r}_j, \quad (4)$$

where

$$G(\vec{r}_i, \vec{r}_j) = \langle Bb | V_{ij} | Aa \rangle_{ij} \quad (5)$$

is the integration over all other spatial coordinates and the spin and isospin matrix elements. The subscript ij appearing on the matrix element in Eq. (5) means that \vec{r}_i and \vec{r}_j are being held fixed. To solve Eq. (5) we need an explicit form of V_{ij} . The ⁶Li ground state is well described in the l - s coupling scheme as ¹³S and the ⁶He ground state as ³¹S, so that the two states differ in their spin and isospin. Therefore, the central part of the interaction V_{ij} which contributes is the Majorana potential

$$V_{ij} = (\vec{\sigma}_i \cdot \vec{\sigma}_j) (\vec{t}_i \cdot \vec{t}_j) V(\vec{r}_i - \vec{r}_j). \quad (6)$$

Tensor forces can also contribute but are much less important.^{3,7,8} Exchange terms can be treated approximately by renormalizing the potential [Eq. (6)]. Substituting Eq. (6) into Eq. (5), the most

general solution of $G(\vec{r}_i, \vec{r}_j)$ is

$$\begin{aligned} G(\vec{r}_i, \vec{r}_j) &= \langle Bb | (\vec{\sigma}_i \cdot \vec{\sigma}_j) (\vec{t}_i \cdot \vec{t}_j) V(\vec{r}_i - \vec{r}_j) | Aa \rangle_{ij} \\ &= \sum_{\substack{L, l \\ M, m}} S_{L, l}^{M, m} Y_L^{M*}(\hat{r}_j) Y_l^m(\hat{r}_i) V(\vec{r}_i - \vec{r}_j) \\ &\quad \times \mathcal{R}_B(r_j) \mathcal{R}_b(r'_i) \mathcal{R}_A(r_j) \mathcal{R}_a(r'_i). \end{aligned} \quad (7)$$

The $\mathcal{R}(r)$ are the one-dimensional radial wave functions of the single nucleons. [In general the angular and radial dependence of the wave functions are not separable, and it is implicitly understood that $\mathcal{R}(r)$ may depend on L and l .] The variables r and r' are measured relative to the center of mass of the target and projectile, respectively, i.e.,

$$\vec{r}' = \vec{r} - \vec{R}. \quad (8)$$

The constants $S_{L, l}^{M, m}$ are obtained by multiplying Eq. (7) by $Y_L^M(r_j) Y_l^m(r'_i)$ and integrating over $d^2\Omega_j d^2\Omega_i$:

$$S_{L, l}^{M, m} = \langle Bb | (\vec{\sigma}_i \cdot \vec{\sigma}_j) (\vec{t}_i \cdot \vec{t}_j) Y_L^M(\hat{r}_j) Y_l^m(\hat{r}_i) | Aa \rangle_{r_j r_i}. \quad (9)$$

Here the subscripts r_i and r_j indicate that the one-dimensional radial integrals have been removed. From Eq. (9) it is apparent that L and l are the angular momenta transferred to particles j and i , respectively. For (⁶Li, ⁶He) reactions the internal wave functions of a and b are approximately ¹³S and ³¹S, thus no angular momentum is transferred to particles i , and $l = 0$:

$$\begin{aligned} G(\vec{r}_i, \vec{r}_j) &= \frac{1}{4\pi} \sum_{L, M} S_L^M Y_L^{M*}(\hat{r}_j) V(\vec{r}_i - \vec{r}_j) \\ &\quad \times \mathcal{R}_B(r_j) \mathcal{R}_b(r'_i) \mathcal{R}_A(r_j) \mathcal{R}_a(r'_i), \end{aligned} \quad (10)$$

$$S_L^M = \langle Bb | (\vec{\sigma}_i \cdot \vec{\sigma}_j) (\vec{t}_i \cdot \vec{t}_j) Y_L^M(\hat{r}_j) | Aa \rangle_{r_i r_j}. \quad (11)$$

We wish to substitute Eq. (10) into Eq. (4) and solve for $F(\vec{R})$. As the solution stands now, it is impractical because a six-dimensional integral must be solved for each value of \vec{R} . The computation can be reduced considerably by making the six-dimensional integral [Eq. (4)] dependent only upon the magnitude of \vec{R} and not upon its direction. To accomplish this we rotate the coordinate system so that the vector \vec{R} points along a new z axis. The old z axis is assumed to be the beam direction.

Such a rotation gives⁹:

$$F(\vec{R}) = \frac{1}{4\pi} \sum_{L, M} \left[Y_L^{M*}(\theta_R, 0) \sum_{i,j} S_L^M f_L(R) \right], \quad (12)$$

$$f_L(R) = \int \mathcal{R}_B(r_j) \mathcal{R}_b(r'_i) V(\vec{r}_i - \vec{r}_j) P_L(\theta_{Rj}) \mathcal{R}_A(r_j) \mathcal{R}_a(r'_i) d^3r_j d^3r_i, \quad (13)$$

where θ_R is the angle \vec{R} makes with the incident beam direction and

$$\cos\theta_{Rj} = \frac{\vec{r}_j \cdot \vec{R}}{r_j |R|} . \quad (14)$$

The sum over i and j in Eq. (12) can be considered as a weighted sum over shell model configurations.

Equation (12) is also valid in the original reference frame with the z axis along the incident beam direction because $Y_L^M(\theta_R, 0)$ is unchanged when rotated back to the original frame of reference. The original rotation is made to allow us to use symmetry arguments⁹ to factor the angular dependence out of the six-dimensional integral. The new integral [Eq. (13)] does not depend on the angular orientation of R , and furthermore it can be reduced trivially to a five-dimensional integral by integrating over $d\phi_j$ or $d\phi_i$. The integrand depends simply on the difference of these two angles. The remaining five-dimensional integral must be solved numerically. If one expands the wave functions and the interaction into a sum of Gaussians, one can obtain an analytic solution which is given in Appendix A.

The two general properties of $f_L(R)$ are⁹:

(1) $f_L(R)$ decreases rapidly with increasing L . This results in a predominance of small L transfers for a quasielastic reaction. The strong L dependence is caused by the $P_L(\theta_{Rj})$, which is in the

as (see Appendix B):

$$S_L^M = \sum_{k,I} (-1)^{k+L+1} \frac{1}{3} \left[\frac{(2k+1)(2I+1)}{(2J_B+1)(2T_A+1)} \right]^{1/2} \langle 11 T_B \mu_B | T_A \mu_A \rangle \langle 1 M_a J_A M_A | I(M_a + M_A) \rangle \langle L M I(M_a + M_A) | J_B M_B \rangle \quad (16)$$

$$\times \begin{Bmatrix} L & K & 1 \\ J_A & I & J_B \end{Bmatrix} \langle J_b = 0, T_b = 1 | \sum_i t_i \sigma_i | J_a = 1, T_a = 0 \rangle_{r_i} \langle J_B T_B | \sum_j t_j [\sigma_j \times Y_L(\hat{r}_j)]^k | J_A, T_A \rangle_{r_j} .$$

The cross section is proportional to $|S_L^M|^2$ and is therefore proportional to $\langle B | | \sum_j t_j [\sigma_j \times Y_L(\hat{r}_j)] | | A \rangle_{r_j}^2$. For $L=0$ the cross section is proportional to $\langle B | | \sum_j t_j \sigma_j | | A \rangle_{r_j}^2$, which is the Gamow-Teller strength. $f_L(R)$ is nearly independent⁹ of the single particle configurations in the target A and residual nucleus B and therefore can be calculated without knowing the configurations of A and B . In the absence of spin-orbit or other spin nonconserving potentials the different angular momenta transferred in the reaction are decoupled and add incoherently. By assuming an incoherent sum of the amplitudes for various angular momenta transferred one can fit the measured angular distributions and easily extract the $L=0$ cross section, which is simply and directly proportional to the Gamow-Teller strength. For a 0^+ target, all final states with $L=0$ cross sections are 1^+ states.

integrand. The $P_L(\theta_{Rj})$ decreases as θ_{Rj} deviates from zero and then oscillates from positive to negative values. The decrease at small angles is proportional to L and upon integration results in a smaller value of $f_L(R)$ for larger L . There would be no L dependence if θ_{Rj} was constrained to be zero, which is the case for a point projectile with a zero range interaction. Both the size of the projectile and the range of the interaction contribute to the L dependence, but in our situation the large size of the ${}^6\text{Li}$ nucleus dominates the L dependence, making it considerably stronger than in $({}^3\text{He}, t)$ or (p, n) .

(2) $f_L(R)$ is only weakly dependent upon the shell model configurations of the nucleon j , assuming that all important contributions come from one major shell (for example $2s, 1d$). This is particularly true at the values of R where most of the reaction takes place. It is therefore a good approximation to factor $f_L(R)$ out of the sum \sum_{ij} and include the sum in the matrix element S_L^M . This gives

$$S_L^M = \langle Bb | \sum_{ij} (\vec{\sigma}_i \cdot \vec{\sigma}_j) (\vec{t}_i \cdot \vec{t}_j) Y_L^M(\hat{r}_j) | Aa \rangle_{r_i r_j} . \quad (15)$$

S_L^M contains essentially all of the nuclear structure information. It can be factored into matrix elements for the projectile and target and rewritten

If the target has nonzero spin, then one must know the spin of the final nucleus in order to extract the Gamow-Teller strength.

We should emphasize, however, that the correlation between the $L=0$ cross section of a quasielastic reaction and the Gamow-Teller strength is not perfect because of a very weak dependence of $f_L(R)$ on the nuclear structure configurations. The relative error in the correlation should be less than 10% for the strongest Gamow-Teller transitions, but the percentage error can be expected to increase for some weaker transitions which involve a near cancellation of two large matrix elements.

The preceding theory is for a quasielastic process but, as pointed out by Madsen,¹⁰ even two-step stripping and pickup (or vice versa) reactions may have a simple proportionality between

TABLE I. ${}^6\text{Li}$ elastic scattering potential parameters using volume absorption.

Target	V (MeV)	r^a (fm)	a (fm)	W (MeV)	r_w^a (fm)	a_w (fm)
${}^6\text{Li}$	53.1	2.35	0.524	12.5	2.45	0.673
${}^{18}\text{O}$	385.5	1.05	0.741	15.1	2.04	0.797
${}^{26}\text{Mg}^b$	174.5	1.39	0.646	35.4	1.27	1.26
${}^{42}\text{Ca}^c$	250.0	1.20	0.804	16.0	1.83	0.87
${}^{48}\text{Ca}$	245.0	1.00	0.912	15.6	1.85	0.801

^a Multiplied by $(A_T)^{1/3}$.

^b Also used for mass 30 and mass 34.

^c Also used for mass 44.

the Gamow-Teller strength and the $L=0$ part of the cross section. We will therefore analyze our data assuming this proportionality exists and compare the Gamow-Teller strengths which we extract with those measured from the β decay. In other words, the analysis which we use will assume a quasielastic process, but it is not mandatory that the reaction be quasielastic to extract useful information about the Gamow-Teller strength.

The optical potentials used in the DWBA analysis were taken from other sources^{4,12} except for

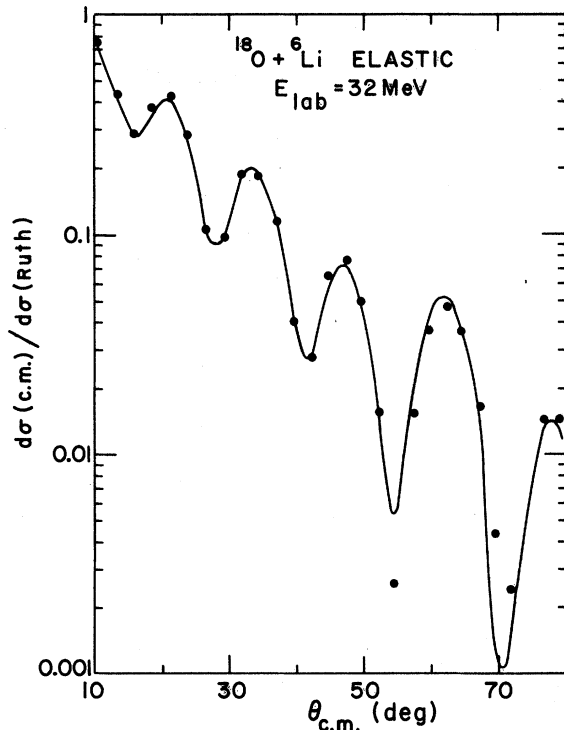


FIG. 3. The ${}^{18}\text{O} + {}^6\text{Li}$ elastic angular distribution at $E_{\text{lab}} = 32$ MeV. The optical model fit is given by the solid line. The parameters for the fit are given in Table I.

${}^{18}\text{O}$ and are given in Table I. The fit we obtain for the ${}^{18}\text{O}$ elastic scattering is shown in Fig. 3. Except for the ${}^6\text{Li}({}^6\text{Li}, {}^6\text{He}){}^6\text{Be}$ reaction,³ the magnitude of the DWBA cross sections is, for our purposes, sufficiently insensitive to the optical potentials. Different sets of optical potentials rarely caused variations of more than 30% in the cross sections. Our form factors and DWBA cross sections are consistent with calculations made by others,^{6,8,11} but are inconsistent with the calculations of Duham *et al.*¹³

Using a Yukawa potential of range 1 fm, the radial dependence of the interaction in Eq. (6) is

$$V(\vec{r}_i - \vec{r}_j) = V_{\sigma T} \frac{e^{-|\vec{r}_i - \vec{r}_j|}}{|\vec{r}_i - \vec{r}_j|}.$$

Duham *et al.* require an interaction strength $V_{\sigma T} \approx 180$ MeV to reproduce their ${}^{26}\text{Mg}({}^6\text{Li}, {}^6\text{He}){}^{26}\text{Al}$ cross sections, which compares to our value of $V_{\sigma T} \approx 30$ MeV using the same wave functions and optical potential. Furthermore, their value of $V_{\sigma T}$ is *larger* than the value they obtained when using a point projectile.⁴ Increasing the size of the projectile should definitely increase the cross section, allowing for a *smaller* value for $V_{\sigma T}$.

IV. REACTION PROCESS

In examining our data, we see that the qualitative characteristics of a quasielastic process are generally and consistently present, but that a careful quantitative analysis indicates the (${}^6\text{Li}$, ${}^6\text{He}$) reaction is not predominantly quasielastic but must be proceeding through multistep processes. Four aspects of the data are examined: (1) the selectivity of populating final states, (2) the angular distributions, (3) the magnitude of the cross sections, and (4) the forbidden $0^+ \rightarrow 0^+$ transitions.

The (${}^6\text{Li}$, ${}^6\text{He}$) reactions can be very selective, as is illustrated in Fig. 4, showing a spectrum of the ${}^{44}\text{Ca}({}^6\text{Li}, {}^6\text{He}){}^{44}\text{Sc}$ reaction at $E_{\text{lab}} = 34$ MeV. Although there are at least 13 known states below 0.98 MeV excitation in ${}^{44}\text{Sc}$, only two or three of these states are strongly excited in ${}^{44}\text{Ca}({}^6\text{Li}, {}^6\text{He}){}^{44}\text{Sc}$. The other states are an order of magnitude weaker. In particular the 2^+ , 4^+ , and 6^+ states at 0.0, 0.350, and 0.271 MeV, respectively, are weakly excited. These states are thought to be mostly pure $(\pi f_{7/2}, \nu f_{7/2}^3)_J$ configurations. In a quasielastic reaction we would expect these states to be weakly populated, since the $\langle || t(\sigma \times Y_L) || \rangle$ matrix element between a pure $(\nu f_{7/2}^4)_{0^+}$ state and a pure $(\pi f_{7/2}, \nu f_{7/2}^3)_J$ state is zero when J is an even integer. The same kind of selectivity is seen also in ${}^{48}\text{Ca}({}^6\text{Li}, {}^6\text{He}){}^{48}\text{Sc}$.⁶

A quasielastic process should also show a strong angular momentum selectivity, resulting in weak-

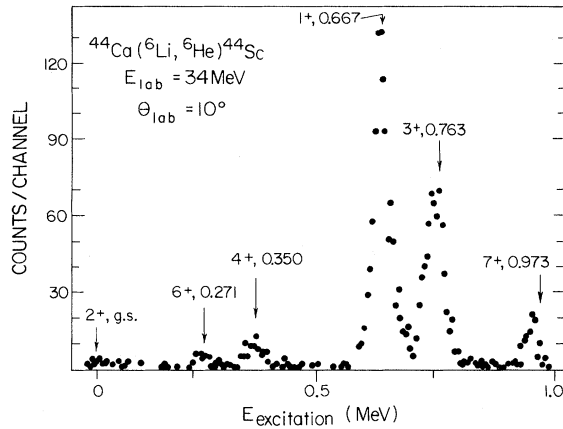


FIG. 4. A spectrum of the $^{44}\text{Ca}(^6\text{Li}, ^6\text{He})^{44}\text{Sc}$ reaction at $E_{\text{lab}} = 34$ MeV and $\theta_{\text{lab}} = 10^\circ$.

er cross sections for higher angular momentum transfers. In particular, the angular distributions should show strong selectivity in angular momentum transfer. For a $0^+ \rightarrow J^+$ transition where J is an odd integer, two angular momentum trans-

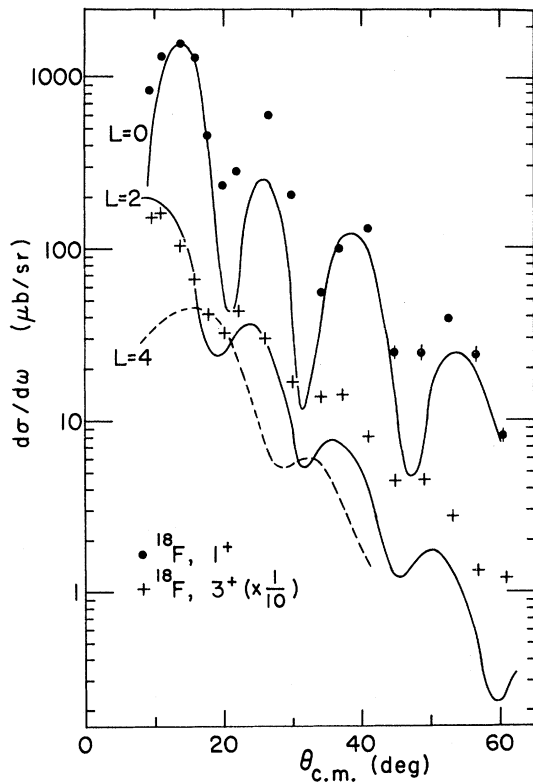


FIG. 5. Angular distributions for the $^{18}\text{O}(^6\text{Li}, ^6\text{He})^{18}\text{F}$ reaction at $E_{\text{lab}} = 32$ MeV populating the 1^+ ground state and the 3^+ state at 0.94 MeV. The lines through the data are arbitrarily normalized DWBA calculations for $L = 0, 2,$ and 4 .

fers, $L_< = J - 1$ and $L_> = J + 1$, are allowed. If the $\langle || t(\sigma \times Y_L) || \rangle$ matrix element is not very small for $L_<$, then the angular distribution should be completely dominated by $L_<$. This is usually found to be true even though the higher $L_>$ results in better angular momentum matching between the incoming and outgoing distorted waves. An example is shown in Fig. 5. The ^{18}F 1^+ state has an $L = 0$ angular distribution and definitely not $L = 2$. The ^{18}F 3^+ has an $L = 2$ angular distribution rather than $L = 4$. For other examples, see Refs. 4, 6, and 7. By strong contrast, the $(^3\text{He}, t)$ reactions consistently show angular distributions characteristic of $L_>$ to these same states.^{14,15}

The most important test of the reaction mechanism is the magnitude. To study the magnitude of the cross sections we choose a Yukawa interaction of range 1 fm for $V(\vec{r}_i - \vec{r}_j)$ given in Eq. (6) and adjust the strength $V_{\sigma\tau}$ to give the measured cross section. If the reaction is quasielastic the strength $V_{\sigma\tau}$ should stay the same for all transitions. The main uncertainty in this procedure is that we do not know the reduced matrix element $\text{RME} = \langle || t(\sigma \times Y_L) || \rangle$ for each transition. For this reason we have only considered the reactions $^{18}\text{O}-$

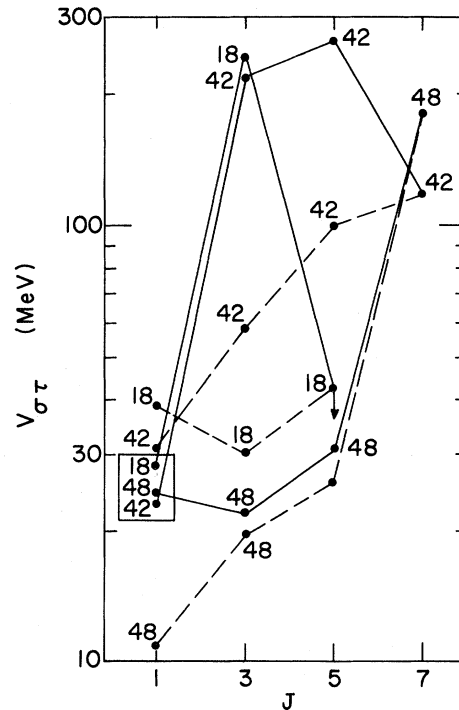


FIG. 6. $V_{\sigma\tau}$ plotted vs J for transitions to the lowest $1^+, 3^+, 5^+,$ and 7^+ states in mass 18, 42, and 48. The solid lines are the $V_{\sigma\tau}$ using RME from realistic shell model calculations. The dashed lines are the $V_{\sigma\tau}$ using the RME of pure configurations.

(${}^6\text{Li}$, ${}^6\text{He}$) ${}^{18}\text{F}$, ${}^{42,48}\text{Ca}({}^6\text{Li}, {}^6\text{He}){}^{42,48}\text{Sc}$ which are near closed shells. The shell-model wave functions should be relatively simpler than for those in the middle of the s - d shell and consequently should be better understood. The $V_{\sigma\tau}$ are shown in Fig. 6 for the lowest 1^+ , 3^+ , 5^+ , and 7^+ transitions. The dashed lines are the values of $V_{\sigma\tau}$ assuming pure $d_{5/2}$ configurations in mass 18 and pure $f_{7/2}$ configurations in mass 42 and mass 48. The solid lines are the values of $V_{\sigma\tau}$, assuming the published wave functions of realistic shell model calculations.^{6,16,17} $V_{\sigma\tau}$ is far from being constant and in general is much too high for the higher spin states. This is a strong indication that the angular momentum selectivity predicted by a quasielastic process is absent. The ${}^{48}\text{Ca}({}^6\text{Li}, {}^6\text{He}){}^{48}\text{Sc}$ results look very similar to the ${}^{48}\text{Ca}({}^3\text{He}, t){}^{48}\text{Sc}$ results,¹⁸ which are believed to go by two-step processes.² This appears to contradict the angular distribution data, which suggests that there is an angular momentum selectivity. The other observation to make is that the $V_{\sigma\tau}$ seems to vary a lot with mass except for the 1^+ transitions (shown by the box in Fig. 6). We will study these 0^+ to 1^+ transitions in greater detail in the next section. Quantitatively, Fig. 6 is very damaging evidence against a quasielastic process.

Attempts have been made to understand (${}^6\text{Li}$, ${}^6\text{He}$) reactions in terms of a two-step (${}^6\text{Li}$, ${}^7\text{Li}$)(${}^7\text{Li}$, ${}^6\text{He}$) neutron pickup, proton stripping reaction.¹³ Such analyses must first understand the cross sections of the 0^+ to 0^+ transitions, which are one-step forbidden. The (${}^6\text{Li}$, ${}^6\text{He}$) reactions have a spin transfer of 1 which requires $L=1$ for 0^+ to 0^+ transitions, but a quasielastic process with a local interaction must satisfy the parity selection rule

$$\pi_{\text{initial}} \pi_{\text{final}} = (-1)^L. \quad (17)$$

Therefore, a quasielastic process should not allow a 0^+ to 0^+ transition. However, there are exchange terms which result from the antisymmetrization of the nucleons in the projectile with the nucleons in the target. The exchange terms are mostly local and result in a renormalization of $V_{\sigma\tau}$, but there is a small nonlocality¹⁹ which can violate Eq. (17) and allow a 0^+ to 0^+ transition. Calculations¹⁹ indicate that the nonlocality contribution is negligibly small.

The most likely explanation of 0^+ to 0^+ transitions is that they proceed through two-step processes.¹³ The 0^+ to 0^+ transitions are valuable for an understanding of two-step processes and their relative importance. We have measured three 0^+ to 0^+ transitions between analog states (Fig. 7). As expected, all 0^+ to 0^+ transitions appear to have pure $L=1$ angular distributions.

The 0^+ to 0^+ transitions are an order of magnitude or more weaker than the strongest 0^+ to 1^+ transitions, and it is difficult to make any quantitative conclusions about the importance of multi-step processes without detailed multistep calculations. One problem is that it is not obvious which multistep processes are and are not important.

V. CORRELATION WITH THE GAMOW-TELLER STRENGTH

We have already stated that the $L=0$ cross section should be proportional to the Gamow-Teller strength for a quasielastic process and also, perhaps, for two-step pickup and stripping processes. To see how good the correlation is we have measured angular distributions for twelve 0^+ to 1^+ transitions for which the Gamow-Teller strength is known from the β decay. Some of these results have already been published.²⁰ From the angular distributions we extract the $L=0$ part of the cross section and, using a DWBA calculation, obtain the RME $|\langle B || \sum \sigma\tau || A \rangle|$. In the DWBA calculation we assume a Yukawa interaction of range 1 fm

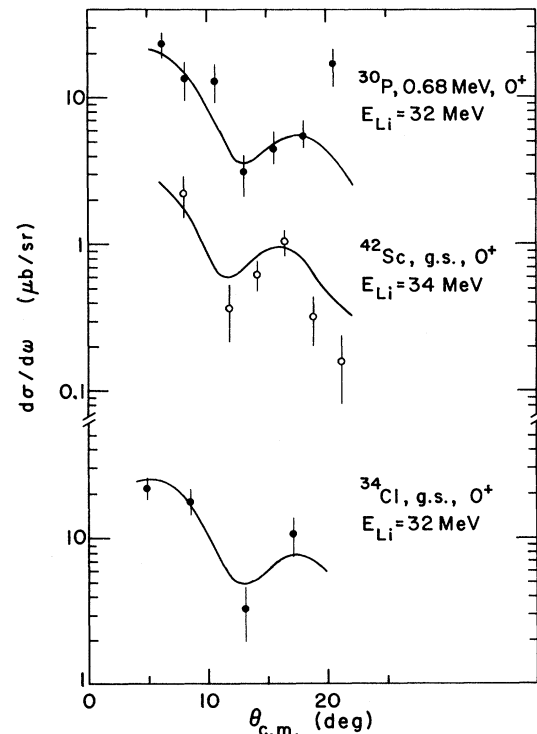


FIG. 7. Angular distributions for the ${}^{30}\text{Si}({}^6\text{Li}, {}^6\text{He}){}^{30}\text{P}$ (0^+ at 0.677 MeV) and the ${}^{34}\text{S}({}^6\text{Li}, {}^6\text{He}){}^{34}\text{Cl}$ (0^+ ground state) reactions at $E_{\text{lab}} = 32$ MeV, and the ${}^{42}\text{Ca}({}^6\text{Li}, {}^6\text{He}){}^{42}\text{Sc}$ (0^+ ground state) reaction at $E_{\text{lab}} = 34$ MeV. The lines through the data are arbitrarily normalized DWBA calculations with angular momentum transfer of $1\hbar$.

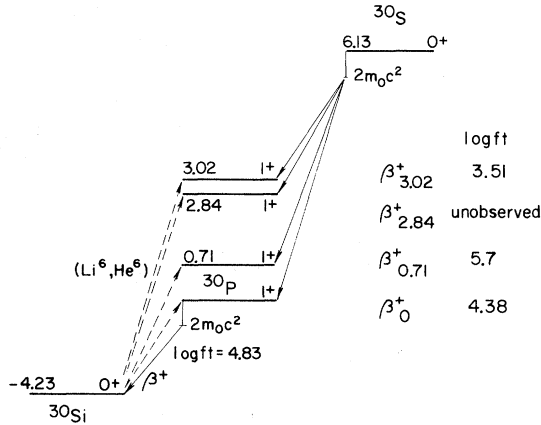


FIG. 8. A level diagram showing the $^{30}\text{Si}(^6\text{Li}, ^6\text{He})^{30}\text{P}$ reaction and the Gamow-Teller β decay in mass 30.

and strength 25 MeV. Then we consider the β decay of the final 1^+ state, if it is the ground state, to the initial 0^+ ground state of the target and from the ft value extract the RME according to the equations

$$ft = \frac{6250 \text{ sec}}{1.51 \langle M_{GT} \rangle^2}, \quad (18)$$

$$\langle M_{GT} \rangle^2 = \frac{1}{2(2J_A + 1)(2T_B + 1)} \times \left[\langle T_A T_{ZA} 1 \pm 1 | T_B T_{ZB} \rangle \langle B || \sum_j \sigma_j t_j || A \rangle \right]^2. \quad (19)$$

If the final 1^+ state is not a ground state, then we consider the β decay to this 1^+ state from the 0^+ , $T_Z = -1$ analog of the 0^+ , $T_Z = 1$ target, as is shown in Fig. 8.

Using this procedure, we find the following correlation:

$$\frac{d\sigma^{L=0}}{d\Omega_{\text{expt}}} \approx N_A^2 \langle A || \sum_j t_j \sigma_j || B \rangle^2 \frac{d\sigma^{L=0}}{d\Omega_{\text{DWBA}}}, \quad (20)$$

where $d\sigma^{L=0}/d\Omega_{\text{DWBA}}$ is part of the DWBA calculation which depends upon the spins of A and B and the Q value but not upon the microscopic nuclear structure. N_A is a normalization constant which should be nearly unity and equal for all transitions if the reaction is quasielastic. Experimentally we find that N_A is not the same for all transitions but is rather smoothly dependent upon the mass of the target A . The observation that N_A is essentially independent of the final nucleus B demonstrates that a correlation exists between the $L=0$ part of the $(^6\text{Li}, ^6\text{He})$ cross sections and the Gamow-Teller strength.

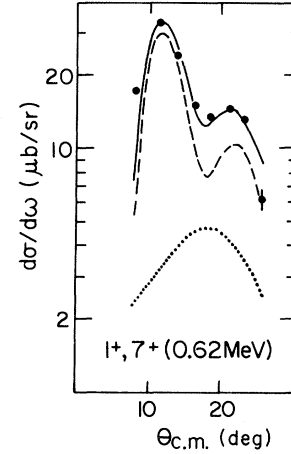


FIG. 9. The angular distribution for the $^{42}\text{Ca}(^6\text{Li}, ^6\text{He})^{42}\text{Sc}$ reaction at $E_{\text{lab}} = 34$ MeV to the unresolved 1^+ and 7^+ doublet at 0.62 MeV. DWBA calculations for the 1^+ with $L=0$ (dashed line) and for the 7^+ with $L=6$ (dotted line), and the incoherent sum (solid line) are shown.

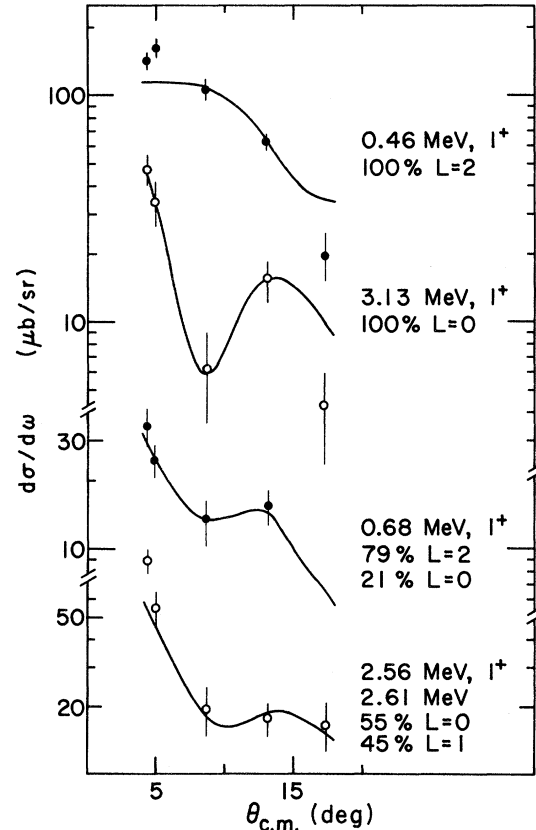


FIG. 10. Angular distributions for the $^{34}\text{S}(^6\text{Li}, ^6\text{He})^{34}\text{Cl}$ reaction at $E_{\text{lab}} = 32$ MeV to the four lowest 1^+ states in ^{34}Cl . The lines through the data are the incoherent sum of DWBA calculations with different angular momentum transfers. The percentages of the integrated cross section for each L transfer are shown.

TABLE II. A comparison of the Gamow-Teller strength obtained from (${}^6\text{Li}$, ${}^6\text{He}$) reactions and β decay.

Final state E_x (MeV)	$\frac{d\sigma}{d\Omega}$ (First max.) ($\mu\text{b/sr}$)	$ \langle B \parallel \sum \sigma\tau \parallel A \rangle $ (${}^6\text{Li}$, ${}^6\text{He}$)	β decay
${}^6\text{He}$ (0)	77	5.5	5.6
${}^{18}\text{F}$ (0)	1550	6.3	4.6
${}^{26}\text{Al}$ (1.06)	210	5.4	2.7
${}^{30}\text{P}$ (0)	220	5.9	1.0
(0.709)	($L=2$)	<1.8	0.22
(2.84)	($L=2$)	<2.1	<1.0
(3.02)	70	9.9	2.8
${}^{34}\text{Cl}$ (0.46)	($L=2$)	<1.0	0.35
(0.68)	~ 10	1.6	0.64
(2.56)	~ 12	5.3	1.4
(3.13)	16	9.7	3.0
${}^{42}\text{Sc}$ (0.62)	30	4.8	4.0

It is most significant that apart from any calculation, a simple look at the 0^+ to 1^+ angular distributions gives a correct qualitative understanding of the Gamow-Teller strength. The angular distributions of the six transitions with the largest Gamow-Teller strength show nearly pure $L=0$ shapes, while the three transitions with the smallest Gamow-Teller strength show nearly pure $L=2$ shapes. These angular distributions are shown in Figs. 5, 9, and 10, and Refs. 3, 4, and 20. A compilation of the RME is given in Table II. The first column gives the differential cross section at the first maximum in the $L=0$ part of the angular distribution. The second and third column give the RME obtained from the (${}^6\text{Li}$, ${}^6\text{He}$) cross

sections (with $N_A=1$) and the β decay, respectively. It is quite evident from looking at mass 30 and 34 that a good correlation with the β decay exists for the relative strengths of the eight transitions. If we consider all 12 transitions, there appears to be a smooth mass dependence. This mass dependence is plotted in Fig. 11. It is difficult to conclude much from only six mass points, but the ratio appears to show a shell effect, being quite large in the middle of the s - d shell.

The (${}^6\text{Li}$, ${}^6\text{He}$) cross sections are dominated by a strong Q -value dependence. The less negative the Q value is, the stronger the cross section. Hence the ${}^{18}\text{F}$ 1^+ state has the largest cross section, since it has the least negative Q value. The Q value becomes more negative, on the average, as A increases. This is true because of the increased Coulomb energy in going from a $T_z=+1$ nucleus to a $T_z=0$ nucleus. It is most satisfying that the DWBA apparently has removed this strong Q -value dependence. To exhibit the correlation between the Gamow-Teller strength and the $L=0$ cross sections in mass 30 and 34, it is most important that the strong Q -value dependence of the cross section be removed. A 3 MeV more negative Q value results in approximately a factor of 9 smaller cross section. This explains why the states near 3 MeV excitation in ${}^{30}\text{P}$ and ${}^{34}\text{Cl}$ have small cross sections although they have a large RME. The strong Q -value dependence goes away as the incident bombarding energy is increased. This is an important reason why (${}^6\text{Li}$, ${}^6\text{He}$) reactions must be studied at higher energies.

To clarify some points let us take a critical look at our analysis. We have assumed a direct one-step quasielastic reaction with only the Majorana force for the inelastic interaction. We have neglected exchange terms and the tensor force. We feel that a more sophisticated "quasielastic" calculation is unwarranted because the reaction is probably not entirely quasielastic and is almost certainly dominated by multistep processes in the middle of the $2s$ - $1d$ shell where the cross sections are much too large.

The inclusion of exchange terms will increase our calculated cross sections but will not alter significantly the shapes of the angular distributions.^{3,8} Furthermore, the percentage of contribution of the exchange terms to the cross section is nearly independent of the target and final nucleus. There will be a small target mass dependence from recoil corrections but this should be negligible. Our value for $V_{\sigma\tau} = 25$ MeV is already unrealistically high, and the inclusion of exchange terms would allow us to obtain the same cross sections with a value of $V_{\sigma\tau}$ closer to the ~ 10 MeV obtained from free nucleon-nucleon potentials.

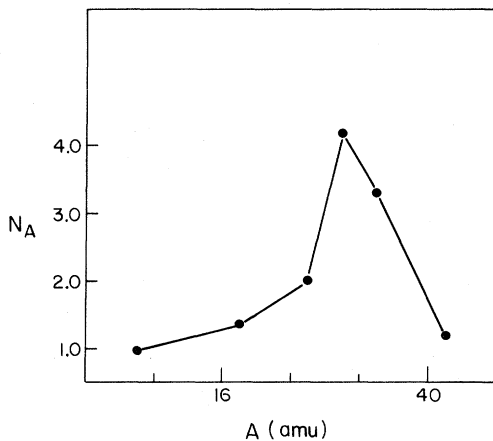


FIG. 11. The ratio of the Gamow-Teller matrix elements extracted from the (${}^6\text{Li}$, ${}^6\text{He}$) reactions divided by the Gamow-Teller matrix elements extracted from the ft values of β decay. The ratio, which is the parameter N_A in Eq. (20), is plotted vs mass.

The inclusion of the tensor force also will not change our results significantly. In the ${}^6\text{Li}$ - $({}^6\text{Li}, {}^6\text{He}){}^6\text{Be}$ reaction, the contribution of the tensor force is less than 20% of the total cross section.³ For 0^+ to 1^+ transitions it will be a factor of 5 weaker according to spin statistics. This is borne out by calculations.^{7,8} It is easy to show that for 0^+ to 1^+ transitions the angular distribution of the tensor contribution will be mostly $L=2$ in shape. This, of course, means that the $L=0$ part of the cross section and its correspondence with the Gamow-Teller strength will be unaffected by the tensor force.

The major weakness of our calculation is that we assume a quasielastic process when it is probable that other processes are more important. The correspondence between the $L=0$ part of the cross section and the Gamow-Teller strength must be considered no more than an empirical observation. We certainly have not explained the full story of why this correlation exists.

VI. DISCUSSION

It is safe to conclude from our analysis that the $({}^6\text{Li}, {}^6\text{He})$ reactions have sizable contributions from multistep processes. The most convincing evidence for multistep processes is the lack of preference for small angular momentum transfer. The cross sections to high spin states are much larger than is predicted by a quasielastic process. This is exemplified in Fig. 6. Even among 1^+ states, the $L=2$ contribution to the cross section is sizable in $A=30$ and 34 , indicating that multistep processes are important. A quasielastic process predicts that the total $L=2$ strength to all 1^+ states should be less than 10% of the total $L=0$ strength. Experimentally the $L=2$ strength is approximately equal to the $L=0$ strength in mass 30 and 34.

The presence of multistep processes undoubtedly are the cause of the strange mass dependence of N_A , shown in Fig. 11. The effect is strong, resulting in 0^+ to 1^+ cross sections which are more than an order of magnitude too large in $A=30$ and 34 . Nevertheless, there remains a good correlation between the $L=0$ cross section and the Gamow-Teller strength even in $A=30$ and 34 . We are fortunate that multistep processes do not destroy the correlation. Madsen's suggestion¹⁰ that a two-step pickup-stripping reaction may be a valuable spectroscopic tool is apparently and unexpectedly becoming a reality in the $({}^6\text{Li}, {}^6\text{He})$ reaction.

One may then ask the question, why does $({}^6\text{Li}, {}^6\text{He})$ work when $({}^3\text{He}, t)$ fails to work? Madsen's crucial assumption is that the intermediate states which contribute to a two-step pro-

cess must be at nearly the same energy. This seems like a plausible assumption if the intermediate states with large nuclear structure overlap with the initial and final states also have good matching conditions with the incoming and outgoing distorted waves. In a two-step process $({}^3\text{He}, \alpha)(\alpha, t)$ the high binding energy of the intermediate α results in a lot of kinetic energy. There is a bad angular momentum mismatch between the intermediate state and the initial and final states. The result is that contributions off the energy shell become important and Madsen's argument is no longer valid. A possible intermediate state for $({}^6\text{Li}, {}^6\text{He})$ is ${}^7\text{Li}$, which should have good matching conditions for most transitions.

It becomes clear that $({}^6\text{Li}, {}^6\text{He})$ should now be seriously considered as a tool for measuring the Gamow-Teller strength. Knowledge of the distribution of Gamow-Teller strength over excitation energy would be valuable in understanding nuclear structure and the spin dependence of nuclear forces. Experimentally, all that is known about the distribution of Gamow-Teller strength comes from the β -decay transitions (mostly in light nuclei) which are energetically allowed. Theoretically, large shell-model calculations, particularly in the middle of the s - d shell, do poorly in predicting the distribution of Gamow-Teller strength.^{20,21}

The hindrance of allowed β decay in heavy nuclei (with large neutron excess) clearly indicates that both the Fermi and Gamow-Teller strength lie at higher excitation.²² The Fermi strength has been found to be concentrated in a single state, the isobaric analog state of the parent. It remains to be found to what extent the Gamow-Teller strength is concentrated and at what excitation energy this concentration occurs. It is likely, both from shell-model calculations and the meager experimental data that most of the Gamow-Teller strength lies above the analog state.²³ Hardy's²⁴ experiment on the proton emission of ${}^{33}\text{Cl}$ following β decay of ${}^{33}\text{Ar}$, suggests a narrow concentration of Gamow-Teller strength at 8 MeV excitation in ${}^{33}\text{Cl}$, which is a full $2\frac{1}{2}$ MeV above the analog state. We have already used the ${}^{48}\text{Ca}({}^6\text{Li}, {}^6\text{He})$ - ${}^{48}\text{Sc}$ reaction²⁵ to map out the Gamow-Teller strength up to 6.4 MeV excitation in ${}^{48}\text{Sc}$. Our analysis suggests that approximately 88% of the Gamow-Teller strength lies at higher energies. In a shell-model calculation, the excitation energy of the Gamow-Teller strength is proportional to the magnitude of the Majorana force $V_{\sigma\tau}(\vec{\sigma}_i \cdot \vec{\sigma}_j) \times (\vec{t}_i \cdot \vec{t}_j)$ between the particles and holes. In nuclear structure calculations one is unsure what strength to use for $V_{\sigma\tau}$. A measurement of the distribution of Gamow-Teller strength will be

TABLE III. The parameters g and b used in a Gaussian expansion of the ⁶Li and ⁶He single particle wave functions and a Yukawa of range 1 fm (unit distance=1 fm).

	$g_{1 \text{ or } 4}$	$b_{1 \text{ or } 4}$	g_2	b_2	g_3	b_3
⁶ Li	1.0	0.165 578 9	0.133 223 5	0.061 431 2	0.009 161 1	0.022 387 5
⁶ He	1.0	0.141 378 0	0.144 703 0	0.046 076 7	0.014 975 6	0.014 530 4
Yukawa	6.608 7 0.094 444	26.015 8 0.093 975	1.711 30	3.666 6	0.519 41	0.780 95

valuable in determining $V_{\sigma\tau}$. Of equal interest is the degree to which the Gamow-Teller strength is localized. The measurement of so-called spreading width of a giant Gamow-Teller resonance would be of great value for understanding nuclear structure. It is our conclusion that the (⁶Li, ⁶He) reaction holds the promise of answering these questions and the reaction should be pursued at higher beam energies to allow the study of higher excitations in nuclei.

APPENDIX A: ANALYTIC SOLUTION OF $f_L(R)$ IN EQ. (12)

Let us expand each radial wave function into a sum of Gaussians of the form

$$\mathcal{R}_a(r) = r^{l_a} \sum_a g_a e^{-b_a r^2}, \quad (\text{A1})$$

where l_a is the angular momentum of the single particle state, and g_a and b_a form a set of adjustable parameters. Single particle wave functions with zero or one node (not counting nodes at $r=0$

or ∞) can be well described out to about 16 fm by a sum of 3 Gaussians. If we properly normalize the wave function such that

$$\int \mathcal{R}_a^2(r) r^2 dr = 1, \quad (\text{A2})$$

then

$$\mathcal{R}_a(r) = \frac{2(l_a/2+1)}{\pi^{1/4} [(2l+1)!!]^{1/2}} N_a r^{l_a} \sum_a g_a e^{-b_a r^2}, \quad (\text{A3})$$

where

$$N_a^2 = \frac{1}{\sum_{j,k} g_j g_k (b_j + b_k)^{-(3/2+l_a)}}. \quad (\text{A4})$$

Let us also expand the interaction into a sum of Gaussians:

$$V(\vec{r}_i - \vec{r}_j) = V_{\sigma\tau} \sum_s g_s e^{-b_s (\vec{r}_i - \vec{r}_j)^2}. \quad (\text{A5})$$

If we substitute these Gaussian expansions for the wave functions and interaction potential into Eq.

(13) we get

$$f_L(R) = \frac{8^2 N_a N_b N_B V_{\sigma\tau}}{3\pi^2 [(2l_A+1)!! (2l_B+1)!!]^{1/2}} \sum_{\substack{a,A \\ b,B,s}} g_a g_A g_b g_B g_s \int r_i^2 r_j^{2l} (\vec{r}_i - \vec{R})^2 e^{-(b_A+b_B)r_j^2} e^{-(b_a+b_b)(\vec{r}_i - \vec{R})^2} \\ \times e^{-b_s (\vec{r}_i - \vec{r}_j)^2} P_L(\theta_{R_j}) d^3 r_j d^3 r_i, \quad (\text{A6})$$

where $l = \frac{1}{2}(l_A + l_B)$ and $l_a = l_b = 1$. The solution of this integral for L as an even integer is:

$$f_L(R) = \frac{32\pi^2 V_{\sigma\tau} N_a N_b N_B}{3 [(2l_A+1)!! (2l_B+1)!!]^{1/2}} \sum_{\substack{a,A \\ b,B \\ s}} \left(g_a g_A g_b g_B g_s \frac{(\beta + b_s)^{l-1} b_s^2 e^{-\alpha_s R^2}}{\beta_s^{2l+5}} \sum_{J=\frac{1}{2}L}^l \left\{ \frac{(l - \frac{1}{2}L)!}{(J - \frac{1}{2}L)!} \frac{(2l+1+L)!!}{(2J+1+L)!!} \frac{1}{(l-J)!} \right. \right. \\ \left. \left. \times \left[\frac{\alpha_s^2 R^2 - 2J\alpha_s}{\gamma_s} + \frac{3}{2} \frac{\beta^2}{(\beta + b_s)\gamma_s} + l - J + \frac{3}{2} \right] (2\gamma_s R^2)^J \right\} \right), \quad (\text{A7})$$

where

$$\beta = b_a + b_b,$$

$$\beta_s^2 = b_s [b_a + b_b + b_B + b_A] + (b_a + b_b)(b_A + b_B),$$

$$\alpha_s = (b_a + b_b)(b_A + b_B) b_s / \beta_s^2, \quad \gamma_s = \frac{\beta^2 b_s^2}{(\beta + b_s) \beta_s^2}.$$

The main advantage of an analytic solution is that one can examine the form factor and gain a better understanding of how different parameters affect it. For the ⁶Li reaction, the most important terms in the summation satisfies the condition $\beta \ll b_s$. Taking this limit into the extreme, it is easy to see that the L and R dependence of $f_L(R)$ is

independent of the range of the force, $1/b_s$. The parameters g and b used for the ${}^6\text{Li}$ and ${}^6\text{He}$ single particle wave functions are given in Table III. They are similar to the ones in Ref. 3. The parameters g_s and b_s are also given for a Yukawa of range 1 fm approximated by a sum of four Gaussians.³ The bound states for the target nucleons are calculated by varying the depth of a Woods-Saxon potential to obtain eigenstates of the correct binding energy. The standard geometry of the potential which we used was $R = 1.25A^{1/3}$,

$a = 0.65$. A spin-orbit term as given by Perez²⁶ was also included but had almost no effect on the form factor.

APPENDIX B: SOLUTION OF S_L^M

$$S_L^M = \langle Bb | \sum_{ij} (\vec{\sigma}_i \cdot \vec{\sigma}_j) (\vec{t}_i \cdot \vec{t}_j) Y_L^M(r_j) | Aa \rangle_{r_i r_j}.$$

Let us define I and T as the channel spin and channel isospin, respectively. Using the Wigner-

Ekhart theorem

$$\begin{aligned} S_L^M = & \sum_{I, I', T, T'} \langle J_b M_b J_B M_B | I' M_I \rangle \langle T_b \mu_b T_B \mu_B | T' \mu' \rangle \langle J_a M_a J_A M_A | I M_I \rangle \langle T_a \mu_a T_A \mu_A | T \mu \rangle \\ & \times (-1)^{I' - M_I'} (-1)^{T' - \mu'} \begin{pmatrix} I' & L & I \\ -M_I' & M & M_I \end{pmatrix} \begin{pmatrix} T' & 0 & T \\ -\mu' & 0 & \mu \end{pmatrix} \\ & \times \langle (J_b J_B) I', (T_b T_B) T' \parallel \sum_{i,j} (\vec{\sigma}_i \cdot \vec{\sigma}_j) (\vec{t}_i \cdot \vec{t}_j) Y_L^M(r_j) \parallel (J_a J_A) I, (T_a T_A) T \rangle_{r_i r_j}. \end{aligned}$$

For (${}^6\text{Li}$, ${}^6\text{He}$) $J_a = 1$, $T_a = 0$, $J_b = 0$, $T_b = 1$. Therefore $I' = J_B$, $T = T_A$, and

$$\begin{aligned} S_L^M = & \sum_I \langle 1 \mu_b T_B \mu_B | T_A \mu_A \rangle \langle 1 M_a J_A M_A | I M_I \rangle (-1)^{J_B - M_B} \frac{1}{(2T_A + 1)^{1/2}} \begin{pmatrix} J_B & L & I \\ -M_B & M & M_I \end{pmatrix} \\ & \times \langle (0 J_B) J_B, (1 T_B) T_A \parallel \sum_{i,j} (\vec{\sigma}_i \cdot \vec{\sigma}_j) (\vec{t}_i \cdot \vec{t}_j) Y_L(r_j) \parallel (1 J_A) I, (0 T_A) T_A \rangle_{r_i r_j}. \end{aligned}$$

The operator can be written

$$(\vec{\sigma}_i \cdot \vec{\sigma}_j) Y_L(r_j) = - \sum_k \left(\frac{2k+1}{2L+1} \right)^{1/2} \{ \sigma_i \times [\sigma_j \times Y_L(r_j)] \}^k \cdot,$$

where k is the total momentum transferred to particle j . The reduced matrix element is then

$$- \sum_k \langle (0 J_B) J_B, (1 T_B) T_A \parallel \sum_{ij} \left(\frac{2k+1}{2L+1} \right)^{1/2} [\sigma_i \times [\sigma_j \times Y_L(r_j)] \}^k \cdot (\vec{t}_i \cdot \vec{t}_j) \parallel (1 J_A) I, (0 T_A) T_A \rangle_{r_i r_j}.$$

Factoring into separate parts for the projectile and the target we get

$$\begin{aligned} - \sum_k \left(\frac{2k+1}{2L+1} \right)^{1/2} [(2J_B + 1)(2L + 1)(2I + 1)]^{1/2} & \begin{pmatrix} 0 & J_B & J_B \\ 1 & J_A & I \\ 1 & k & L \end{pmatrix} (-1)^{T_B + T_A} (2T_A + 1)^{1/2} \begin{pmatrix} 1 & T_B & T_A \\ T_A & 0 & 1 \end{pmatrix} \\ & \times \langle J_b = 0, T_b = 1 \parallel \sum_i t_i \sigma_i \parallel J_a = 1, T_a = 0 \rangle_{r_i} \langle J_B T_B \parallel \sum_j t_j [\sigma_j \times Y_L(r_j)]^k \parallel J_A, T_A \rangle_{r_j}. \end{aligned}$$

S_L^M is then given by Eq. (16) in the text.

- *Work performed under the auspices of the U. S. Atomic Energy Commission.
- †Present address: Department of Physics, Rutgers University, New Brunswick, New Jersey 08903.
- ‡Present address: Department of Physics, Indiana University, Bloomington, Indiana 47401.
- ¹J. D. Anderson, C. Wong, and J. W. McClure, *Phys. Rev.* **126**, 2170 (1962).
- ²W. R. Coker, T. Udagawa, and H. H. Walter, *Phys. Rev. C* **7**, 1154 (1973); *Phys. Lett.* **46B**, 27 (1973), and references therein.
- ³W. R. Wharton, *Phys. Rev. C* **9**, 164 (1974).
- ⁴H. H. Duhm, N. Veta, W. Heinecke, H. Hafner, H. Homeyer, and P. D. Kunz, *Phys. Lett.* **38B**, 306 (1972).
- ⁵Ortec Incorporated, 100 Midland, Road, Oak Ridge, Tennessee 37830.
- ⁶C. Gaarde and T. Kammuri, *Nucl. Phys.* **A215**, 314 (1973).
- ⁷C. Gaarde and T. Kammuri, *Nucl. Phys.* **A209**, 170 (1974).
- ⁸C. Ciangaru, private communication.
- ⁹W. R. Wharton and P. T. Debevec, *Phys. Lett.* **51B**, 447 (1974).
- ¹⁰V. A. Madsen, in *The Two-Body Force in Nuclei*, edited by S. M. Austin and G. M. Crawley (Plenum, New York, 1972).
- ¹¹C. F. Clement and S. M. Perez, *Nucl. Phys.* **A195**, 561 (1972).
- ¹²C. Fink, private communication.
- ¹³H. H. Duhm, H. Hafner, R. Renfordt, M. Goldschmidt, O. Dragun, and K. I. Kubo, *Phys. Lett.* **48B**, 1 (1974).
- ¹⁴Argonne National Laboratory Physics Division Informal Report No. PHY-1970A, January 1970 (unpublished).
- ¹⁵H. H. Duhm, K. Peterseim, R. Seehars, R. Finlay, and C. Détraz, *Nucl. Phys.* **A151**, 579 (1970).
- ¹⁶C. Rolfs, W. E. Kieser, R. E. Azuma, and A. E. Litherland, *Nucl. Phys.* **A199**, 274 (1973).
- ¹⁷T. T. S. Kuo and G. E. Brown, *Nucl. Phys.* **A114**, 241 (1968).
- ¹⁸P. Kossanyi-Demay, P. Roussel, H. Faraggi, and R. Schaeffer, *Nucl. Phys.* **A148**, 181 (1970).
- ¹⁹W. G. Love, *Particles and Nuclei* **3**, 318 (1972).
- ²⁰W. R. Wharton and P. T. Debevec, *Phys. Lett.* **51B**, 451 (1974).
- ²¹P. W. M. Glaudemans, P. M. Endt, A. E. L. Dieperink, *Ann. Phys. (N.Y.)* **63**, 134 (1971).
- ²²Jun-Ichi Fujita, S. Fujii, and K. Ikeda, *Phys. Rev.* **133**, B549 (1964).
- ²³For a general review see M. Morita *et al.*, *Prog. Theor. Phys. Suppl.* **48**, 41 (1971), and references therein.
- ²⁴J. C. Hardy, J. E. Esterl, R. G. Sextro, and J. Cerny, *Phys. Rev. C* **3**, 700 (1971).
- ²⁵P. T. Debevec and W. R. Wharton (unpublished).
- ²⁶S. M. Perez, *Nucl. Phys.* **A136**, 599 (1969).